

AN ABSTRACT OF THE THESIS OF

NGUYEN HOANG THINH for the MASTER OF SCIENCE  
(Name) (Degree)

Electrical and  
in Electronics Engineering presented on April 13 - 1972  
(Major) (Date)

Title: CALCULATION OF AXIAL MODE SEPARATION OF A  
SEMICONDUCTOR LASER FROM REFLECTANCE

SPECTRUM

*Redacted for Privacy*

Abstract approved: \_\_\_\_\_  
Cheng C. Chang

It is reported that the axial mode separation of a semiconductor laser can be computed from the reflectance spectrum of a narrow spectral range near the lasing frequency. The Kramers-Kronig dispersion relation is used in this computation.

GaAs semiconductor laser is taken as an example. The computed values of the normalized frequency separation for GaAs at lasing photon energy of 1.38 eV range from 0.107 to 0.111 for various widths of the reflectance spectrum. These results are in good agreement with the measured ones.

Calculation of Axial Mode Separation of a Semiconductor  
Laser From Reflectance Spectrum

by

Nguyen Hoang Thinh

A THESIS

submitted to

Oregon State University

in partial fulfillment of  
the requirements for the  
degree of

Master of Science

June 1972

APPROVED:

*Redacted for Privacy*

Assistant Professor of Electrical and Electronics  
Engineering

in charge of major

*Redacted for Privacy*

Head of Department of Electrical and Electronics  
Engineering

*Redacted for Privacy*

Dean of Graduate School

Date thesis is presented April 13 - 1972

Typed by Clover Redfern for Nguyen Hoang Thinh

## ACKNOWLEDGMENT

The author wishes to express his deep gratitude to Dr. Cheng C. Chang for his suggestion, guidance and assistance during the course of this work and the writing of this thesis.

Special thanks go to A. I. D. for financial support.

Thanks also go to my wife and our parents for their encouragement.

## TABLE OF CONTENTS

<u>Chapter</u>	<u>Page</u>
I. INTRODUCTION	1
II. REFLECTANCE AND OPTICAL CONSTANTS	4
Relations Among Optical Constants	4
Reflectance of GaAs	6
III. KRAMERS-KRONIG ANALYSIS	10
Kramers-Kronig Dispersion Relation	10
Calculation of the Phase Angle Using an Entire Spectral Range	12
Calculation of the Phase Angle Using a Limited Spectral Range	13
IV. CAVITY AND MODES IN A SEMICONDUCTOR LASER	17
Cavity and Resonant Modes	17
Axial Mode Separation of a Semiconductor Laser	18
V. PROCEDURE OF CALCULATING AXIAL MODE SEPARATION	20
Computation of $L\Delta\nu/c$ Versus Photon Energy Using Conventional Method	20
Computation of $L\Delta\nu/c$ Versus Photon Energy Using Narrow Spectrum Method	22
Computation of $L\Delta\nu/c$ Versus Upper Integration Limit $b$	23
VI. RESULTS AND DISCUSSION	25
BIBLIOGRAPHY	31
APPENDICES	33
Appendix I: Reflectance Data	33
Appendix II: Proof of Equation (3.4)	34
Appendix III: Calculation of the Integrand in Equation (3.3) in the Case $E = E_o$	36
Appendix IV: Symbols and Procedures of Calculation for Program MODSEP1	37
Appendix V: Program MODSEP1	39
Appendix VI: Output of Program MODSEP1	40

<u>Chapter</u>	<u>Page</u>
Appendix VII: Symbols and Procedures of Calculation for Programs MODSEP2A and MODSEP2B	41
Appendix VIII: Program MODSEP2A	43
Appendix IX: Output of Program MODSEP2A	44
Appendix X: Program MODSEP2B	45
Appendix XI: Output of Program MODSEP2B	46
Appendix XII: Upper Integration Limit Data	47

## LIST OF FIGURES

<u>Figure</u>	<u>Page</u>
1A. Reflectance data versus photon energy of GaAs at room temperature.	7
1B. Reflectance data of GaAs (continued).	8
1C. Reflectance data of GaAs (continued).	9
2. Calculated normalized frequency separation $L\Delta\nu/c$ of GaAs laser versus photon energy from the conventional method.	26
3. Calculated normalized frequency separation $L\Delta\nu/c$ of GaAs laser versus photon energy from the narrow spectrum method.	27
4. Calculated normalized frequency separation $L\Delta\nu/c$ of GaAs laser at 1.38 eV versus upper integration limit b.	28
5. Calculated refractive index $n$ of GaAs versus photon energy at room temperature.	30

# CALCULATION OF AXIAL MODE SEPARATION OF A SEMICONDUCTOR LASER FROM REFLECTANCE SPECTRUM

## I. INTRODUCTION

A simple laser cavity consists of two parallel and highly reflecting mirrors, in which there exists a great number of transverse electromagnetic ( $TEM_{mnq}$ ) modes. However for a practical laser, higher order modes are suppressed. As a result, only one or a few fundamental normal modes are sustained.

The allowed modes in a laser that actually oscillate will depend on the gain characteristics of the laser medium, which will depend on the spectral linewidth, i. e. , the spontaneous emission linewidth of the laser transition. Any mode falling outside of the linewidth will not oscillate because of an insufficient gain.

Since the mode separation is small relative to the linewidth, many modes will in fact oscillate. For selecting a single-mode operation sometimes mode selectors (19) will be required in the cavity. Recently Popov and Shuikin (15) used a compound resonator to obtain single-mode emission from a semiconductor.

To design a laser with single mode operation such as the work cited above requires the knowledge of the mode separation. Furthermore it is useful to know the mode separation in determining the gain of a desired mode (8). It follows that the prediction of the mode

separation of a semiconductor laser is very desirable.

In a semiconductor laser, modes are determined by the length and the refractive index  $n$  of the medium. It is known that the refractive index of a semiconducting material is very frequency-sensitive. For predicting mode separation the value of  $n$  versus frequency is usually obtained experimentally. For instance, the mode separation of a GaAs junction laser was measured by Burns, Dill, and Nathan (3). Later Marple (9) measured the refractive index  $n$  versus wavelength  $\lambda$  and computed the mode separation for GaAs laser.

As a matter of fact, those direct measurements of  $n$  and mode separation are not easy. Robinson (16) suggested that the calculation of the optical constants such as the refractive index  $n$ , and the extinction coefficient  $k$  of a material can be made from its reflectance spectrum by using the Kramers-Kronig dispersion relation. The application of this relation required the knowledge of a whole spectral range. Later Roessler (17) suggested a modified approach, which required only a limited range of spectrum.

Since the reflectance spectrum of a semiconductor is easy to obtain experimentally and readily available, attempt has been made to calculate its axial mode separation from the reflectance data. Furthermore, justification of using a narrow reflectance spectrum to obtain the mode separation with reasonable accuracy has also been

made. To the author's knowledge, such an attempt has not been explored.

Due to the frequency-sensitivity of the refractive index  $n$  in a dispersive medium, the calculation of the mode separation requires the knowledge of  $dn/d\nu$ , i. e., the slope of  $n$  versus frequency. The purpose of this work is to show how the quantity  $dn/d\nu$  and hence the mode separation of a semiconductor laser are obtained from a narrow spectral reflectance range around the lasing frequency. Also in this work the change of the calculated results for mode separation as a function of spectral width was also examined. The GaAs junction laser was taken as an example. The value of the mode separation obtained in such a computation was compared to that calculated from the conventional method, i. e., the method using a whole spectral range, and to the measured data as well. As a result, the calculated values of the axial mode separation for GaAs laser were in good agreement with the measured ones.

## II. REFLECTANCE AND OPTICAL CONSTANTS

### Relations Among Optical Constants

When radiation is incident upon the surface of a material, one part is reflected, another is absorbed, and the remainder is transmitted through the material. Approximately the expressions for the reflectance  $R$ , transmittance  $T$ , and absorptance  $A$  at normal incidence are given by (23)

$$R = r^2 \left[ \frac{1 + (1 - r^2) \exp(-2\alpha d)}{1 - r^4 \exp(-2\alpha d)} \right] \quad (2.1)$$

$$T = \frac{(1 - r^2) \exp(-\alpha d)}{1 - r^4 \exp(-2\alpha d)} \quad (2.2)$$

$$A = \frac{(1 - r^2) [1 - \exp(-\alpha d)]}{1 - r^2 \exp(-\alpha d)} \quad (2.3)$$

where  $r = \frac{N-1}{N+1}$  is the Fresnel reflection coefficient at normal incidence with  $N = n - ik$ , the complex refractive index of the crystal,  $\alpha = 4\pi k / \lambda$  the absorption coefficient at normal incidence, and  $d$  the sample thickness. It is easily seen that  $A + R + T = 1$ .

Expressions (2.1) and (2.2) have been widely used for determining the optical properties of solids in many experiments.

Actually, the expression for reflectance was used in the case of  $\alpha d \gg 1$ . For this reason, only the information of the front-surface

reflectance was needed. Thus Equation (2.1) becomes

$$R = |r|^2.$$

The expression for  $r$  can be written as

$$r = \frac{n-ik-1}{n-ik+1} = |r| e^{i\theta} \quad (2.4)$$

Then the magnitude of the measured reflectance is

$$R = |r|^2 = \frac{(n-1)^2 + k^2}{(n+1)^2 + k^2} \quad (2.5)$$

and the phase is

$$\theta = \tan^{-1} \frac{-2k}{n^2 + k^2 - 1} \quad (2.6)$$

Solving for  $n$  and  $k$  in Equation (2.4), one obtains

$$n = \frac{1-R}{1+R-2\sqrt{R} \cos \theta} \quad (2.7)$$

and

$$k = \frac{-2\sqrt{R} \sin \theta}{1+R-2\sqrt{R} \cos \theta} \quad (2.8)$$

The expressions (2.7) and (2.8) show that the quantities  $n$  and  $k$  are functions of the magnitude  $R$  and phase  $\theta$  of reflectance. The variables  $R$  and  $\theta$  are related to each other as will be seen in the next chapter. The study of the behavior of  $R$  for a semiconductor, particularly for GaAs, is as follows.

### Reflectance of GaAs

As stated in the previous chapter, GaAs laser was taken as an example. The reflectance of GaAs at room temperature is shown in Figures 1A, 1B, and 1C. The data tabulated in Appendix I were gathered from the references as quoted in (4, 12, 14, 23).

Three spectral regions are distinguished (13). The first region (Figure 1B) covering up to about 8 or 10 eV is characterized by the sharp structures associated with the band-to-band transitions. The second region (Figure 1C) extending to about 20 eV shows a rapid decrease in the reflectance which is reminiscent of the behavior of certain metals in the ultraviolet region. This is because the valence electrons become unbound and able to perform collective oscillations.

In the third region (Figure 1C) the reflectance again rises indicating the onset of additional optical absorption. This situation can be thought of as the presence of the transitions between filled d bands, lying below the valence band, and empty conduction band states. It should be noted that in Figure 1A the sharp structure covering from 0.03 eV to 0.05 eV is due to the transition in reststrahlen band.

These curves are used as measured data for the mode separation computation.

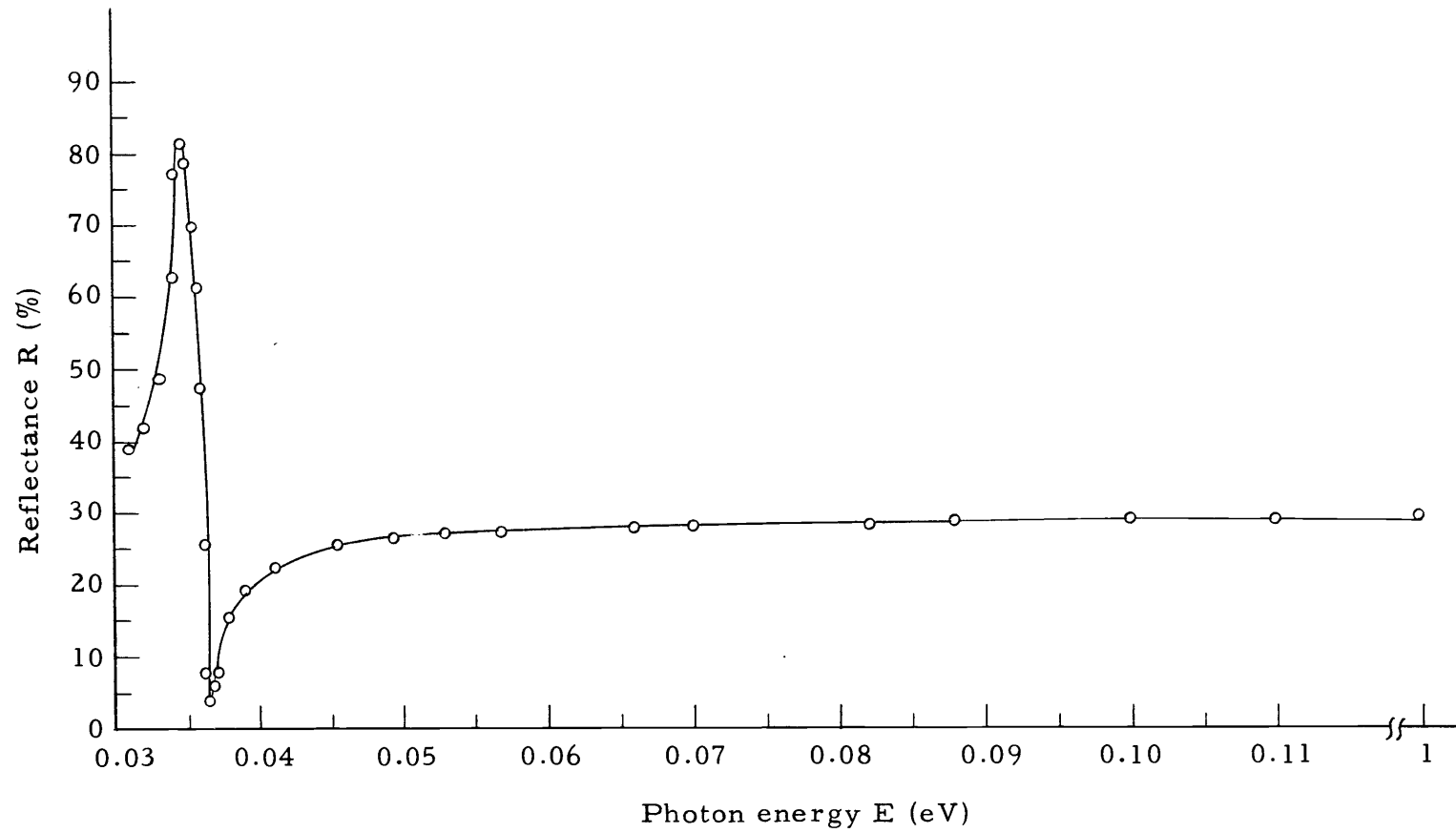


Figure 1A. Reflectance data versus photon energy of GaAs at room temperature.

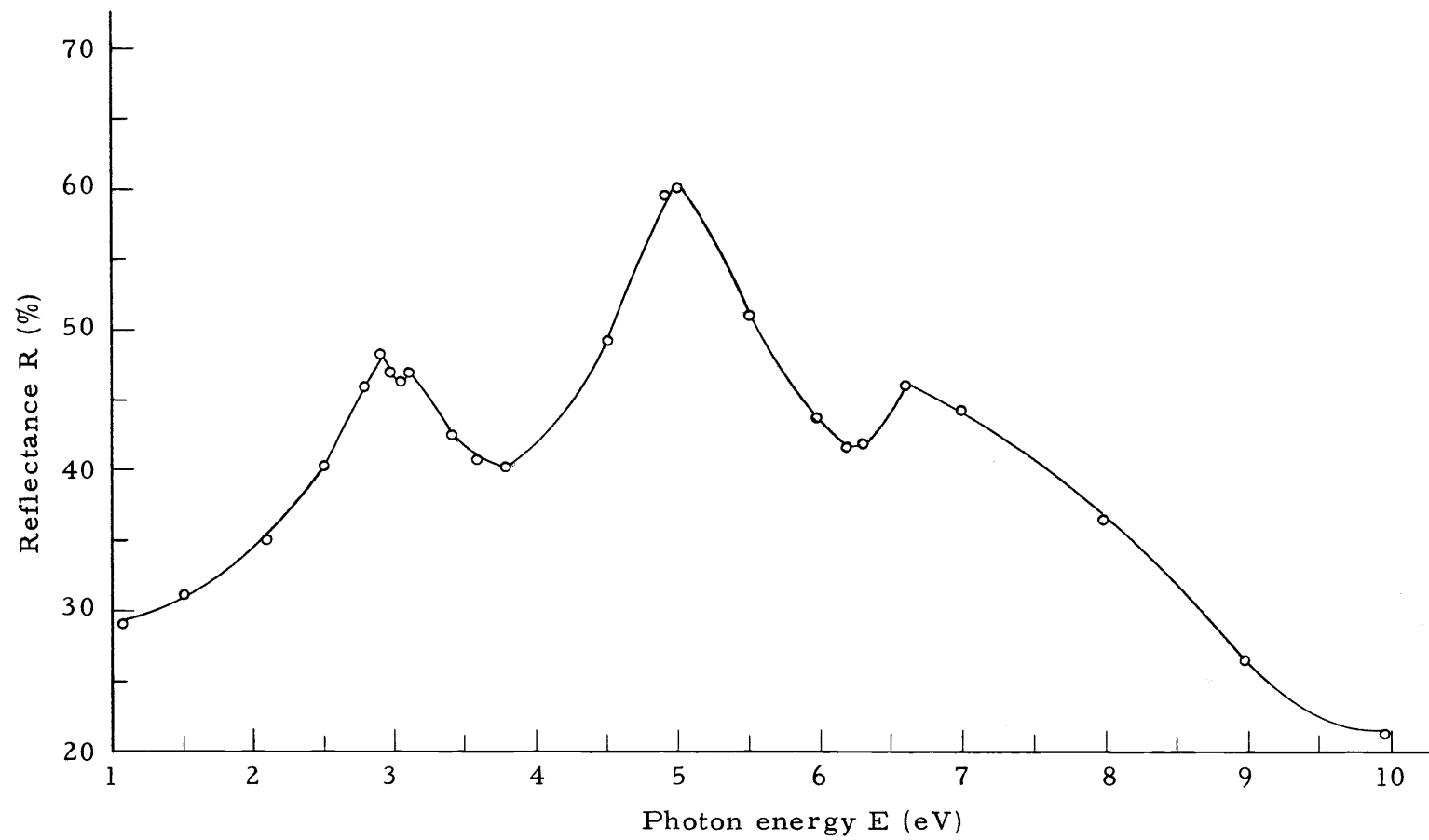


Figure 1B. Reflectance data of GaAs (continued).

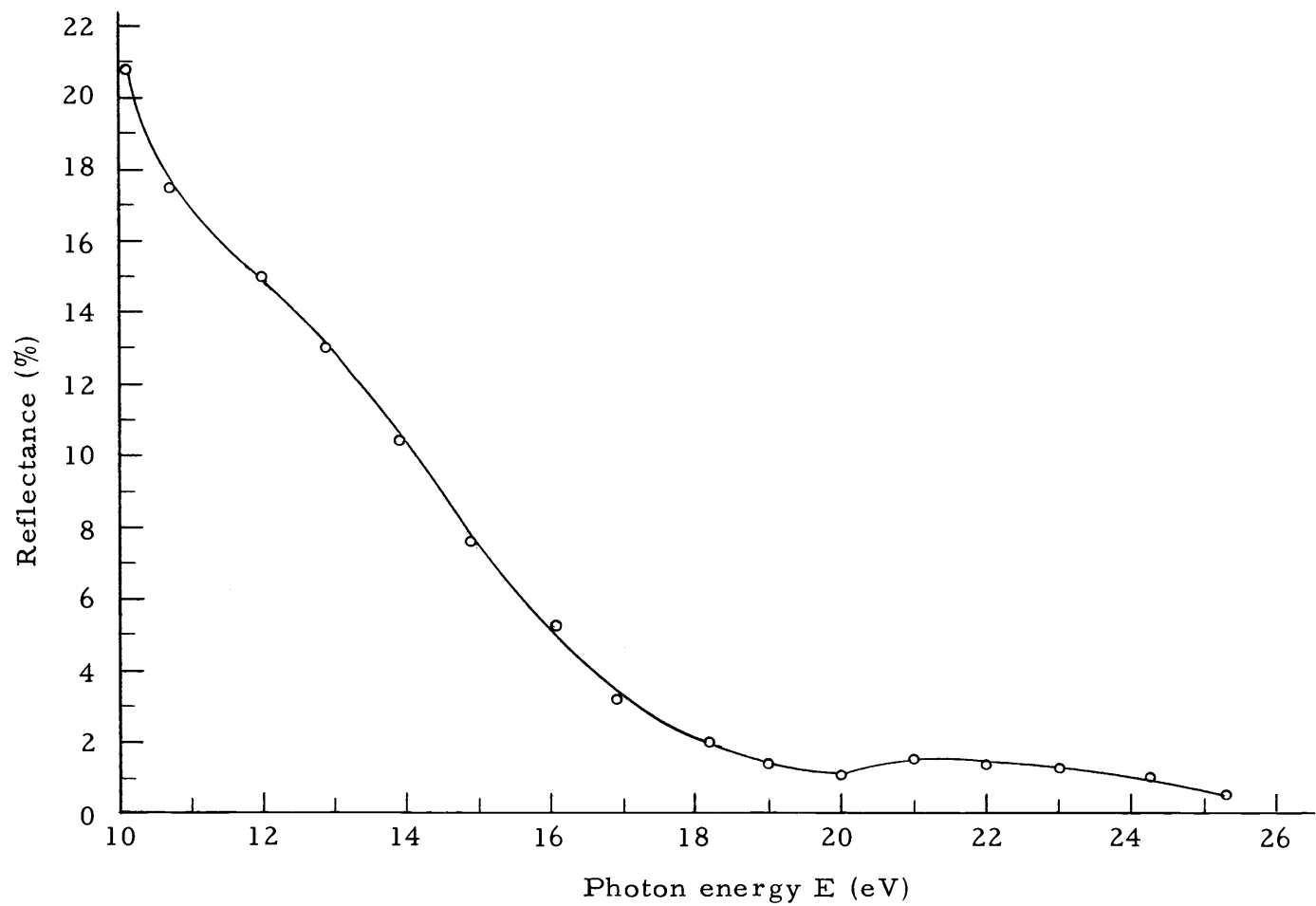


Figure 1C. Reflectance data of GaAs (continued).

### III. KRAMERS-KRONIG ANALYSIS

#### Kramers-Kronig Dispersion Relation

In general the dispersion relation is the relation between the real and imaginary parts of a complex quantity (2). Consequently, the relation between the magnitude and phase of the reflectance is called the dispersion relation or Kramers-Kronig dispersion relation. The application of this relation to reflectance data of normal incidence permits the determination of the refractive index  $n$ , the extinction coefficient  $k$ , and other optical quantities.

Taking the logarithm of both members of Equation (2.4) gives

$$\ln r = \ln |r| + i\theta$$

or

$$\ln r = 1/2 \ln R + i\theta$$

where the relation between  $R$  and  $\theta$  can be written in terms of frequency as (11, 21)

$$\theta(\nu_o) = \frac{\nu_o}{\pi} P \int_0^{\infty} \frac{\ln R(\nu)}{\nu^2 - \nu_o^2} d\nu \quad (3.1)$$

or in terms of photon energy  $E$  as

$$\theta(E_o) = \frac{E_o}{\pi} P \int_0^{\infty} \frac{\ln R(E)}{E^2 - E_o^2} dE \quad (3.2)$$

where  $P$  stands for the Cauchy principal value of the integral.

Equations (3.1) or (3.2) is called Kramers-Kronig dispersion relation.

Accordingly with the knowledge of the reflectance spectrum, the phase angle  $\theta$  can be calculated with a computer. The integral in Equation (3.2) can be represented by a usual one as

$$\begin{aligned}
 \theta(E_o) &= \frac{E_o}{\pi} P \int_0^\infty \frac{\ln R(E)}{E^2 - E_o^2} dE \\
 &= \frac{E_o}{\pi} P \int_0^\infty \frac{\ln R(E) - \ln R(E_o)}{E^2 - E_o^2} dE \\
 &= \frac{E_o}{\pi} \int_0^\infty \frac{\ln R(E) - \ln R(E_o)}{E^2 - E_o^2} dE \quad (3.3)
 \end{aligned}$$

because

$$P \int_0^\infty \frac{dE}{E^2 - E_o^2} = 0 \quad (3.4)$$

The proof of Equation (3.4) is shown in Appendix II.

The integrand in Equation (3.3) is finite for  $E = E_o$  provided the reflectance spectrum does not have an infinite slope at  $E_o$ .

Such infinite slopes are never encountered experimentally.

It is clear that from Equations (3.3) and (3.4) one can see that a constant reflectance gives  $\theta = 0$ .

### Calculation of the Phase Angle Using an Entire Spectral Range

For the evaluation of the phase angle  $\theta$ , in principle, the reflectance data should cover the entire spectral region from zero to infinity. Since the spectral region of the reflectance measurements is always bounded, it is necessary to extrapolate the measured reflectance curve  $R(E)$  to infinite energy in order to compute the integral in Equation (3.3) and hence the refractive index  $n$  in Equation (2.7).

The most reasonable extrapolation procedure assumes that above the valence electron plasma frequency  $\omega_p$  the following expressions are usually used.

$$n^2 - k^2 = 1 - \frac{\omega_p^2}{\omega^2}$$

and

$$2nk = \frac{\omega_p^2 \tau}{\omega^2 \tau^2} \approx 0.$$

These expressions (11) are valid only for  $\omega^2 \tau^2 \gg 1$  and  $\omega > \omega_p$ , where  $\tau$  is the relaxation time of free carriers in the conduction band of a semiconductor.

Thus at high frequencies

$$n \approx 1 - \frac{1}{2} \frac{\omega_p^2}{\omega^2}$$

and

$$R = \frac{(n-1)^2}{(n+1)^2} \approx \frac{1}{16} \frac{\omega_p^4}{\omega^4} \quad (3.5)$$

Therefore if the upper frequency limit of the measurement  $\omega_1$  is larger than  $\omega_p$ , it is logical to extrapolate  $R(\omega)$  beyond  $\omega_1$  by

$$R = R_1 \left( \frac{\omega_1}{\omega} \right)^4$$

or

$$R = (R_1 \omega_1^4) \omega^{-4} \quad (3.6)$$

where  $R_1$  is the measured reflectance at  $\omega_1$ .

On the other hand, for low frequencies the reflectance is approximately constant and hence there is no contribution to  $\theta$  as mentioned in the previous section. Thus no extrapolation for  $R$  to zero frequency is needed.

### Calculation of the Phase Angle Using a Limited Spectral Range

In the case of a limited spectrum, the method described above should be modified to calculate the phase angle  $\theta$ . The modified approach was treated by Roessler (17) as mentioned in the introduction.

In fact, the integral in Equation (3.3) can be broken into three parts as

$$\theta(E_o) = \theta_{0a}(E_o) + \theta_{ab}(E_o) + \theta_{b\infty}(E_o) \quad (3.7)$$

where

$$\theta_{0a}(E_o) = \frac{1}{2\pi} \int_0^a f(R, E_o) dE \quad (3.8)$$

$$\theta_{ab}(E_o) = \frac{E_o}{\pi} \int_a^b \frac{\ln R(E) - \ln R(E_o)}{E^2 - E_o^2} dE \quad (3.9)$$

and

$$\theta_{b\infty}(E_o) = \frac{1}{2\pi} \int_b^\infty f(R, E_o) dE \quad (3.10)$$

where

$$f(R, E_o) = \ln \frac{R(E)}{R(E_o)} \frac{d}{dE} \left( \ln \left| \frac{E+E_o}{E-E_o} \right| \right)$$

Here  $\theta_{ab}(E_o)$  is the contribution from the region of the experimental data,  $\theta_{0a}(E_o)$  and  $\theta_{b\infty}(E_o)$  are not known because of the lack of data. But the integrals  $\theta_{0a}$  and  $\theta_{b\infty}$  can be found as follows.

According to Equation (3.8), in the interval  $(0, a)$ ,  $E$  is everywhere less than  $E_o$  since  $E_o$  lies in  $(a, b)$ . Hence the continuous function  $\frac{d}{dE} \ln \left| \frac{E+E_o}{E-E_o} \right|$  is monotonic with  $E$ .

Thus applying the generalized mean value theorem for integrals to the integral in Equation (3.8) gives

$$\begin{aligned}
\theta_{0a}(E_o) &= \frac{\ln[R(\zeta)/R(E_o)]}{2\pi} \int_0^a \frac{d}{dE} \ln \left| \frac{E+E_o}{E-E_o} \right| dE \\
&= \left[ A - \frac{\ln R(E_o)}{2\pi} \right] \ln \left| \frac{a+E_o}{a-E_o} \right|
\end{aligned} \tag{3.11}$$

where  $A = \ln R(\zeta)/2\pi$  and varies only slowly with  $E_o$ ,  $\zeta$  being some value of  $E$  in the interval  $(0, a)$ .

Similarly, the integral in Equation (3.10) can be written as

$$\begin{aligned}
\theta_{b\infty}(E_o) &= \frac{\ln[R(\eta)/R(E_o)]}{2\pi} \int_b^\infty \frac{d}{dE} \ln \left| \frac{E+E_o}{E-E_o} \right| dE \\
&= \left[ B - \frac{\ln R(E_o)}{2\pi} \right] \ln \left| \frac{b+E_o}{b-E_o} \right|
\end{aligned} \tag{3.12}$$

where  $B = \ln R(\eta)/2\pi$ ,  $\eta$  belonging to the interval  $(b, \infty)$ .

Thus Equation (3.7) has the form

$$\begin{aligned}
\theta(E_o) &= \left[ A - \frac{\ln R(E_o)}{2\pi} \right] \ln \left| \frac{a+E_o}{a-E_o} \right| + \theta_{ab}(E_o) \\
&\quad + \left[ B - \frac{\ln R(E_o)}{2\pi} \right] \ln \left| \frac{b+E_o}{b-E_o} \right|
\end{aligned} \tag{3.13}$$

where the unknown quantities  $A$  and  $B$  may be determined by the fact that the phase angle  $\theta(E_o)$  is zero at energies below the onset of absorption. As a matter of fact theoretically the phase angle  $\theta$

should be zero in regions of no absorption, i. e. , for energies less than the energy gap or  $E = h\nu < E_g$ .

Therefore it is easy to choose two frequencies  $\nu_1$  and  $\nu_2$  such that  $h\nu_{1,2} < E_g$  within the range  $(a, b)$  to obtain two zero  $\theta$ 's.

Consequently, the quantities  $A$  and  $B$  in Equation (3.13) can be solved for the following simultaneous equations

$$\left[ A - \frac{\ln R(E_1)}{2\pi} \right] \ln \left| \frac{a+E_1}{a-E_1} \right| + \theta_{ab}(E_1) + \left[ B - \frac{\ln R(E_1)}{2\pi} \right] \ln \left| \frac{b+E_1}{b-E_1} \right| = 0 \quad (3.14)$$

$$\left[ A - \frac{\ln R(E_2)}{2\pi} \right] \ln \left| \frac{a+E_2}{a-E_2} \right| + \theta_{ab}(E_2) + \left[ B - \frac{\ln R(E_2)}{2\pi} \right] \ln \left| \frac{b+E_2}{b-E_2} \right| = 0 \quad (3.15)$$

where  $E_1 = h\nu_1$  and  $E_2 = h\nu_2$ .

Thus the computation of  $\theta(E_o)$  is essentially as follows:

$R(E)$  is determined experimentally in  $(a, b)$  and, using (3.14) and (3.15), the constants  $A$  and  $B$  are found by computing  $\theta_{ab}(E_1)$  and  $\theta_{ab}(E_2)$ . Then  $\theta(E_o)$  is calculated from Equation (3.13).

#### IV. CAVITY AND MODES IN A SEMICONDUCTOR LASER

##### Cavity and Resonant Modes

A semiconductor laser is usually fabricated with two parallel cleaved surfaces and the other two sawed or roughened. The cavity in a semiconductor laser so obtained is essentially a Fabry-Perot structure. As commonly known, a Fabry-Perot interferometer consists of two optically flat, partially reflecting plates of glass or quartz with their reflecting surfaces held accurately parallel.

Radiation propagating perpendicularly to these reflecting surfaces forms standing waves in the cavity. Standing waves occur whenever the cavity contains an integral number of half-wavelength. For a cavity length  $L$ , this resonance condition is

$$m \frac{\lambda}{2} = L \quad (4.1)$$

where  $m$  is the axial mode number,  $\lambda$  wavelength in air.

Expression (4.1) above is valid for a passive cavity. In a semiconductor laser of refractive index  $n$ , the radiation propagates with wavelength  $\lambda/n$ . Thus, the resonance condition given by Equation (4.1) becomes

$$m \frac{\lambda}{2n} = L$$

or

$$m\lambda = 2nL \quad (4.2)$$

In an actual laser not all the frequencies satisfying Equation (4.2) are permitted to oscillate because of losses due to diffraction, reflection, and absorption. The medium between the mirrors has a net gain that will compensate for these losses. Lower order modes will usually have greater gain than the higher order ones. As a consequence only a few fundamental modes will exist. Furthermore, it is possible to design a laser of single mode operation, i. e. , highly monochromatic light output (15, 19). Such a design requires the knowledge of the mode separation.

#### Axial Mode Separation of a Semiconductor Laser

The refractive index  $n$  of a semiconductor is very frequency-sensitive, i. e. , a function of wavelength. Thus differentiating Equation (4.2) with respect to  $\lambda$  gives

$$\lambda \frac{dm}{d\lambda} + m = 2L \frac{dn}{d\lambda} \quad (4.3)$$

For the separation of two adjacent modes and for large  $m$ , substituting

$$d\lambda \sim \Delta\lambda$$

$$dm = -1$$

$$m = 2nL/\lambda$$

into Equation (4.3), one obtains

$$1 - \frac{\lambda}{n} \frac{dn}{d\lambda} = \frac{1}{2nL} \frac{\lambda^2}{\Delta\lambda}$$

or

$$\Delta\lambda = \frac{\lambda^2}{2L(n - \lambda \frac{dn}{d\lambda})}$$

or in terms of frequency as

$$\Delta\nu = \frac{c}{2L(n + \nu \frac{dn}{d\nu})} \quad (4.4)$$

(by noting that  $\lambda = c/\nu$ ,  $\Delta\lambda = -c\Delta\nu/\nu^2$ ,  $d\nu/d\lambda = -c/\lambda^2$ , and  $dn/d\lambda = (dn/d\nu)(d\nu/d\lambda)$ ), where  $c$  is the velocity of light.

Equation (4.4) can be written as

$$\frac{L\Delta\nu}{c} = \frac{1}{2(n + \nu \frac{dn}{d\nu})} \quad (4.5)$$

or

$$\frac{L\Delta\nu}{c} = \frac{1}{2(n + E \frac{dn}{dE})} \quad (4.6)$$

where  $E$  is the photon energy. The quantity  $L\Delta\nu/c$  can be called the normalized frequency separation of a semiconductor laser.

## V. PROCEDURE OF CALCULATING AXIAL MODE SEPARATION

As mentioned in Chapter I, the GaAs semiconductor laser was taken as an example. The reflectance data of GaAs used here were referred to Chapter II. The Kramers-Kronig dispersion relation was applied to calculate the phase angle  $\theta$  and hence the refractive index  $n$  and the quantity  $dn/dE$  in Equation (4.6). In other words the normalized frequency separation  $L\Delta\nu/c$  of a semiconductor laser was predicted by using the reflectance data through the dispersion relation.

To achieve the calculation of the quantity  $L\Delta\nu/c$ , the conventional method using Equation (3.3) was first used, then followed by the narrow spectrum method, which was derived in Equation (3.13).

### Computation of $L\Delta\nu/c$ Versus Photon Energy Using Conventional Method

As shown in Equation (3.3), this method of calculation requires the whole spectral range from zero to infinity to compute the phase angle  $\theta$ . Practically to calculate the integral in Equation (3.3) with a computer, the upper integration limit of this integral should be finite. In the present work, 50 eV was chosen as this upper limit.

Since the reflectance data of GaAs was not available beyond 25 eV, an extrapolation for  $R(E)$  to 50 eV should be needed. Yet the upper energy limit of 25 eV is larger than the plasma energy

( $\hbar\omega_p \sim 16$  eV) for GaAs (4, 13). Thus the behavior of  $R(E)$  beyond 25 eV has the form of Equation (3.6):

$$R = R_1 \omega_1^4 \omega^{-4}$$

or in terms of energy as

$$R = R_1 E_1^4 E^{-4} \quad (5.1)$$

where  $E_1 = 25$  eV and  $R_1 = 0.006$ .

On the other hand, the lower integration limit was chosen as 0.03 eV instead of 0 eV. This is because below 0.03 eV the reflectance is constant and hence there is no contribution to  $\theta$  as stated in Chapter III.

The Simpson's numerical method (10) was used to handle the integral  $\theta(E_o)$  in Equation (3.3) with the aid of a computer. Since this numerical method requires equal intervals, an interpolation of the reflectance data was needed to obtain a set of equally spaced data points.

The spectrum was divided into 0.001 eV intervals within the reststrahlen region, i. e., from 0.03 eV to 0.05 eV due to the sharp variation of reflectance. The rest of the spectrum extending up to 50 eV was divided into 0.015 eV intervals. Then the Lagrangian formula (10) was used to interpolate the reflectance data points. Since the integrand in Equation (3.3) becomes indeterminate when

$E = E_0$ , it has another form as described in Appendix III.

Then the refractive index  $n$  given by Equation (2.7) was computed. The quantity  $dn/dE$  was hence obtained numerically as

$$\frac{dn_j}{dE} \approx \frac{n_{j+1} - n_{j-1}}{2\Delta E} \quad (5.2)$$

where  $\Delta E$  is the equal energy interval of the spectrum.

Finally the normalized frequency separation  $L\Delta\nu/c$  versus photon energy as expressed in Equation (4.6) was found. All these computations were included in a Fortran program named MODSEP1 (see Appendices IV and V).

#### Computation of $L\Delta\nu/c$ Versus Photon Energy Using Narrow Spectrum Method

The narrow spectrum method was described in detail in the third part of Chapter III. The lower limit  $a$  and upper limit  $b$  of the integral  $\theta_{ab}$  in Equation (3.9) were chosen near the lasing energy  $E = 1.38\text{ eV}$ . Consequently in this computation  $b$  was used as a parameter and  $a$  fixed at  $0.1\text{ eV}$ . In this case  $b$  was chosen as  $2\text{ eV}$  and  $3\text{ eV}$ .

The reflectance data points were interpolated to obtain equally spaced points with equal interval of  $0.015\text{ eV}$  by using 3-point Lagrangian interpolation as stated before.

The integral  $\theta_{ab}$  in Equation (3.9) was then calculated using

Simpson's rule as mentioned in the previous section. To compute the integral  $\theta(E_0)$  in Equation (3.13), the unknown quantities  $A$  and  $B$  were determined first from the Equations (3.14) and (3.15). The quantities  $E_1$  and  $E_2$  in these two equations were chosen to be 0.3 eV and 0.5 eV respectively. These values were actually chosen more or less arbitrarily from any value near and less than the energy gap. As a matter of fact, the values  $E_1$  and  $E_2$  were not sensitive to the resultant  $A$  and  $B$ .

The knowledge of  $\theta(E_0)$  in Equation (3.13) permitted the calculation of the refractive index  $n$ , of  $dn/dE$  and hence of the quantity  $L\Delta\nu/c$  versus photon energy as expressed in Equation (4.6). A program named MODSEP2A (see Appendices VII and VIII) was written to complete those calculations.

#### Computation of $L\Delta\nu/c$ Versus Upper Integration Limit $b$

In this computation the narrow spectrum method was also used to calculate the mode separation at lasing photon energy of 1.38 eV (corresponding to the wavelength of 9000 angstroms) as the upper integration limit  $b$  varied. The reflectance data points were interpolated using the same interval of 0.015 eV.

In computing the integral  $\theta(E_0)$  in Equation (3.13), the lower integration limit  $a$  was chosen as 0.1 eV and the upper integration limit  $b$  varied from 2 eV to 24 eV. Two vanishing  $\theta$ 's

corresponding to  $E_1 = 0.3 \text{ eV}$  and  $E_2 = 0.5 \text{ eV}$  were adopted.

The quantities  $A$  and  $B$  in Equations (3.14) and (3.15) vary with

$b$ . The integral  $\theta_{ab}(E_o)$ , where  $E_o = 1.38 \text{ eV}$ , was calculated similarly by using the Simpson's rule.

As usual, with the knowledge of the phase angle  $\theta$ ,  $n$  and hence the normalized frequency separation  $L\Delta\nu/c$  were calculated as a function of the upper integration limit  $b$ . A program named MODSEP2B (see Appendices VII and X) was written for the calculation.

## VI. RESULTS AND DISCUSSION

Figure 2 shows the calculated normalized frequency separation  $L\Delta\nu/c$  of GaAs laser versus photon energy. This curve is the result obtained from the conventional method of computation. The computer output for Figure 2 is included in Appendix VI. As one can see, the normalized mode separation  $L\Delta\nu/c$  at lasing energy of 1.38 eV is 0.1086.

The calculated values of  $L\Delta\nu/c$  from the narrow spectrum method are shown in Figure 3 which is plotted from the computer output tabulated in Appendix IX. The two curves in this figure correspond to  $b$  of 2 eV and 3 eV. At the lasing energy of 1.38 eV the mode separation  $L\Delta\nu/c$  is 0.107 for  $b = 2$  eV and 0.108 for  $b = 3$  eV. As shown in Figure 3 these two curves are very close to each other and to the curve in Figure 2.

The mode separation  $L\Delta\nu/c$  as a function of  $b$  at lasing photon energy is shown in Figure 4. Appendix XI shows the data of the computer output for this figure. Here the values of  $L\Delta\nu/c$  swing only between 0.107 and 0.111. Consequently the quantity  $L\Delta\nu/c$  does not vary much as the spectral width changes.

For the sake of comparison, the measured values for  $L\Delta\nu/c$  at lasing frequency are searched in the literature. The value  $L\Delta\nu/c$  was reported by Burns, Dill and Nathan (3) to be  $0.114 \pm 0.01$  percent

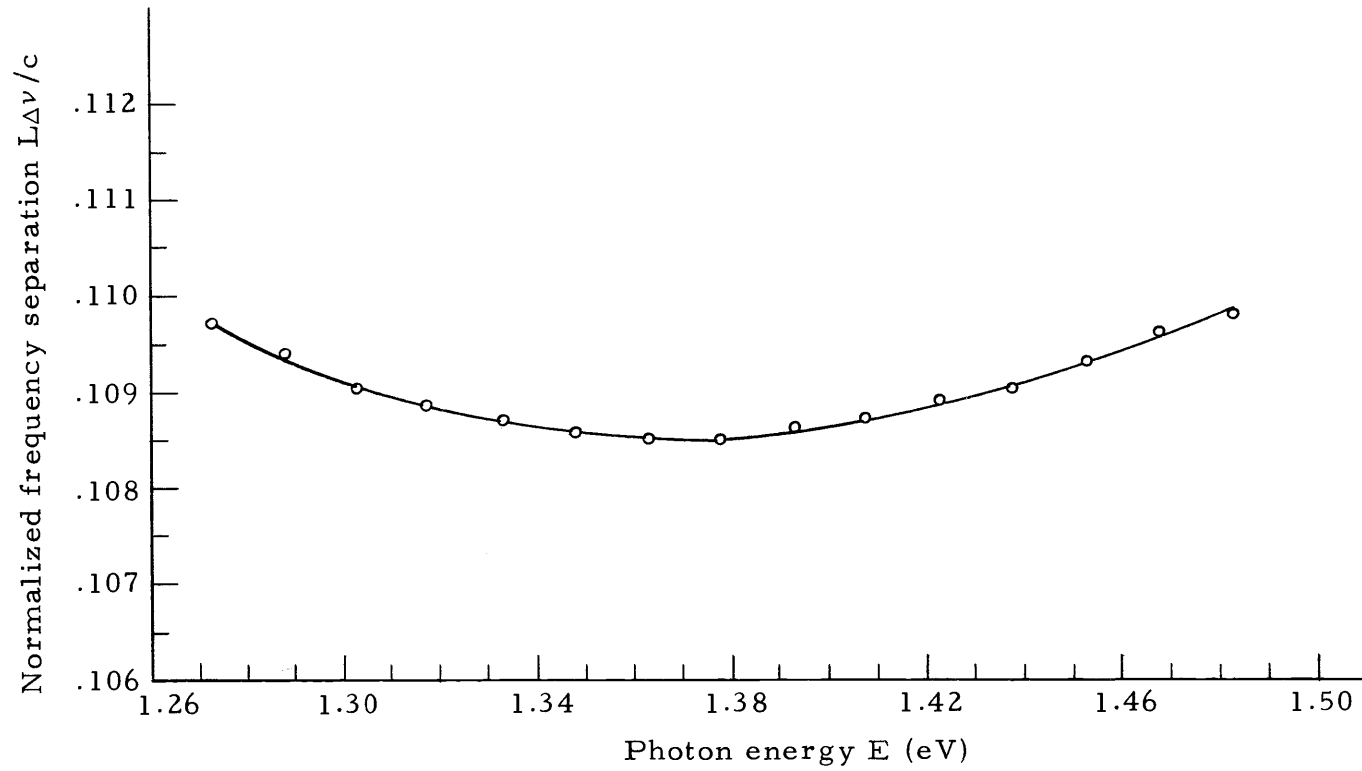


Figure 2. Calculated normalized frequency separation  $L\Delta\nu/c$  of GaAs laser versus photon energy from the conventional method.

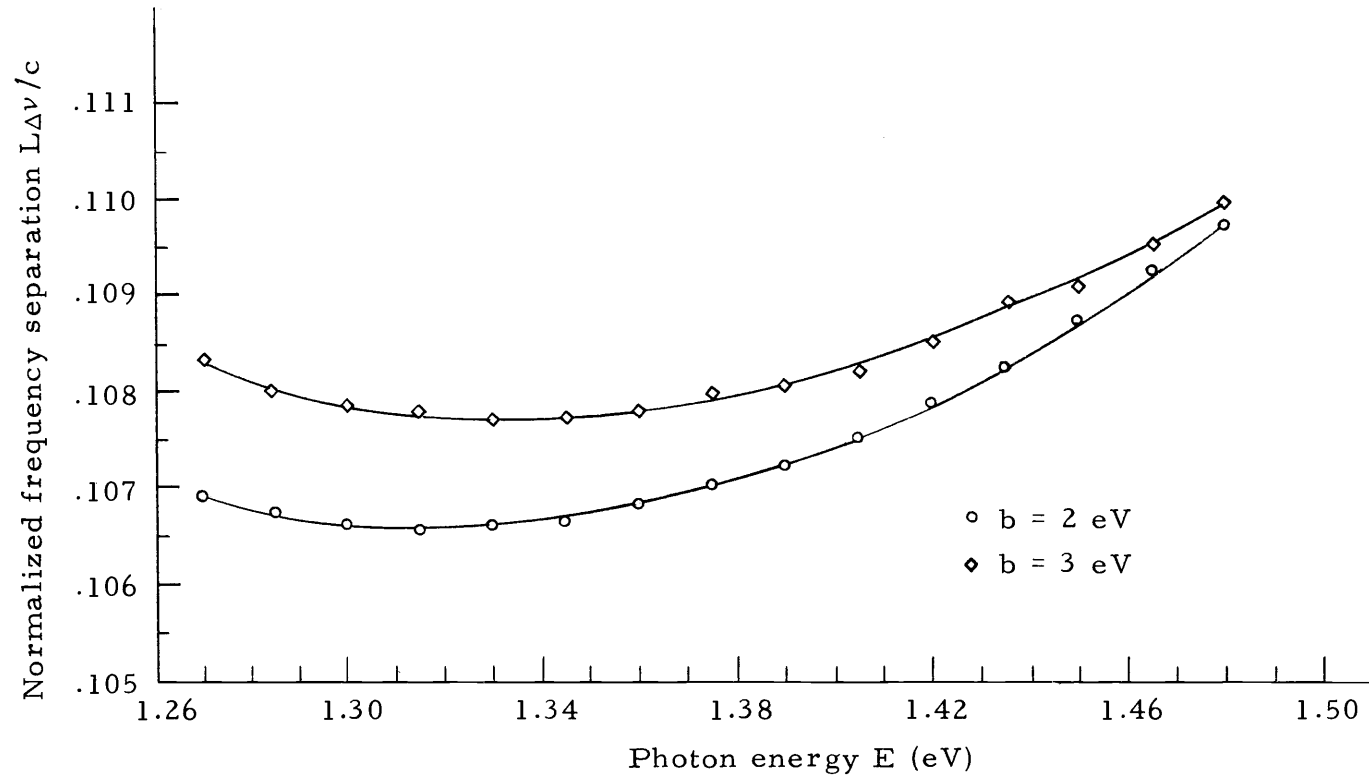


Figure 3. Calculated normalized frequency separation  $L\Delta\nu/c$  of GaAs laser versus photon energy from the narrow spectrum method.

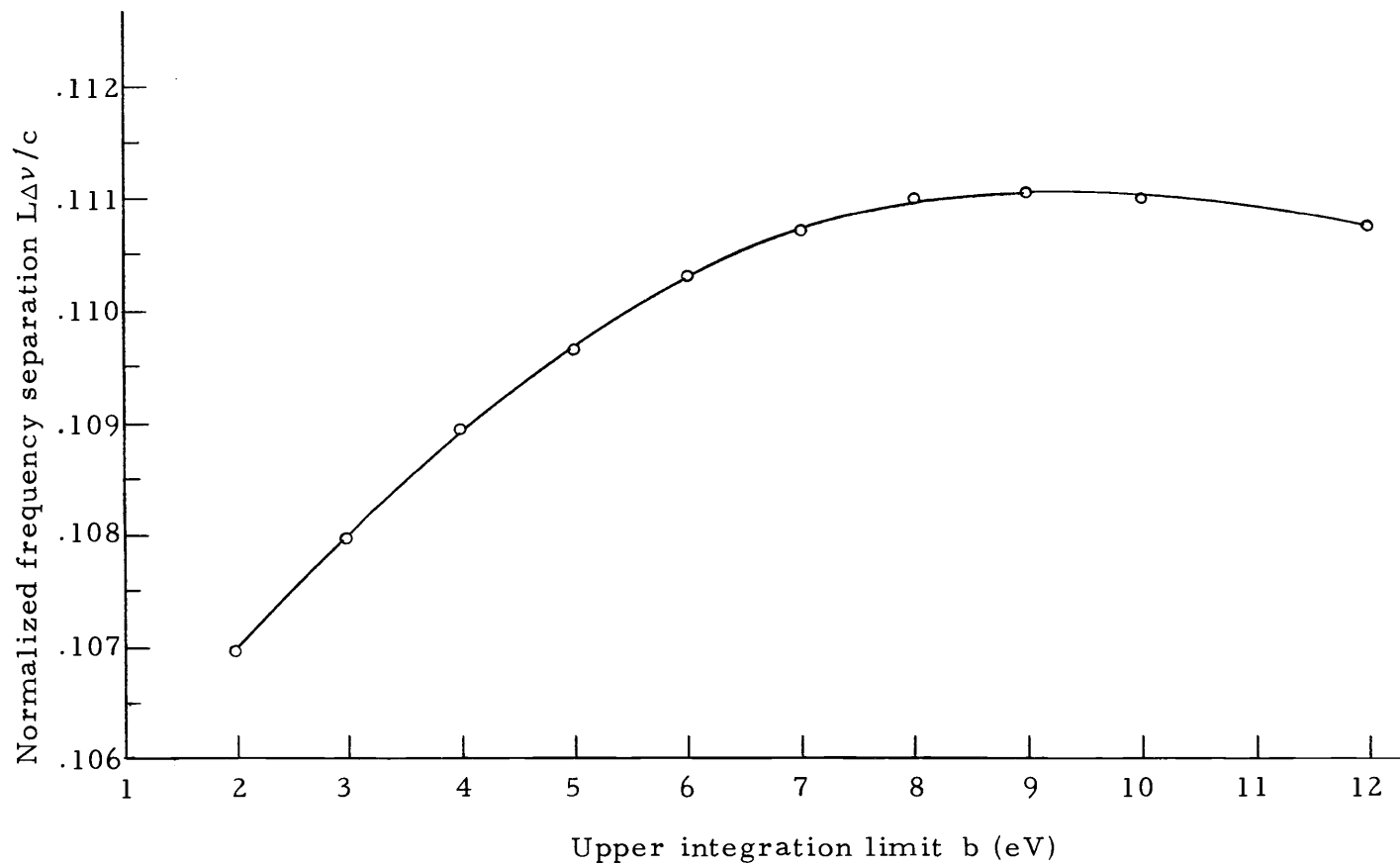


Figure 4. Calculated normalized frequency separation  $L\Delta\nu/c$  of GaAs laser at 1.38 eV versus upper integration limit  $b$ .

and 0.105. Therefore it is reasonable to say that the computed results in this work are in good agreement with the measured ones. The table below shows the comparison between those values.

$L\Delta\nu/c$  at lasing energy of 1.38 eV for GaAs laser

Measured	Computed		
	Conventional Method	Narrow Spectrum Method	
		b = 2 eV	b = 3 eV
0.114 and 0.105	0.1086	0.107	0.108

It is also included that the results for the refractive index  $n$  of GaAs obtained from both methods of computation are shown in Figure 5. These curves are very close to each other, and the computed values for  $n$  agree satisfactorily with the measured ones (9).

In conclusion, in calculating the axial mode separation of a semiconductor laser from reflectance spectrum, the narrow spectrum method has many important advantages. Firstly, this method requires only a narrow spectral range near the energy gap of a semiconductor. Secondly, the set up for measuring such a narrow reflectance spectrum will be much simpler and cost less. In addition, the computing time is tremendously reduced as compared to the conventional method. This work has shown that the narrow spectrum method can be used to compute the mode separation of a semiconductor laser with a reasonable accuracy.

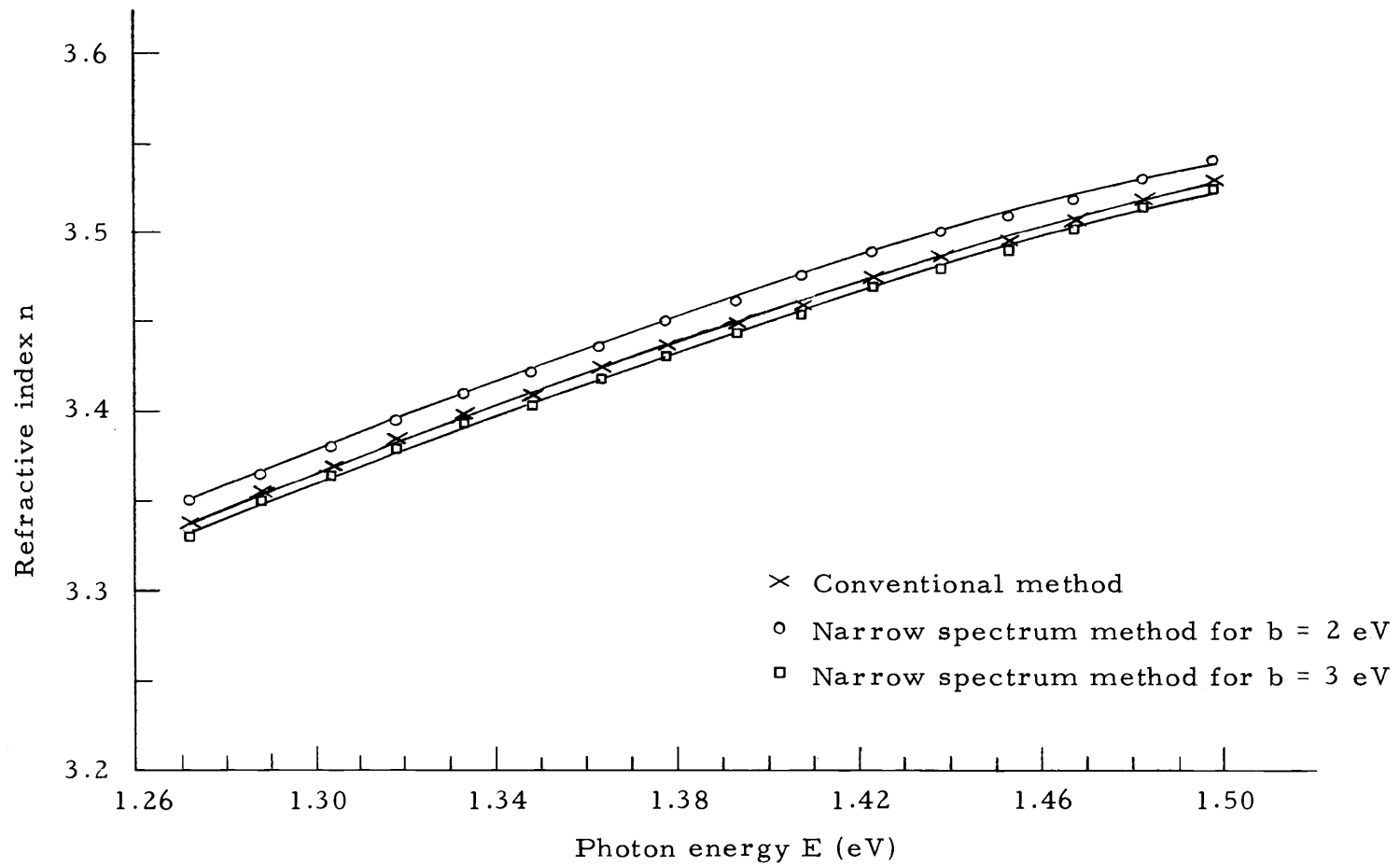


Figure 5. Calculated refractive index  $n$  of GaAs versus photon energy at room temperature.

## BIBLIOGRAPHY

1. Birnbaum, George. Optical masers. New York, Academic Press, 1964. 306 p.
2. Bode, H.W. Network analysis and feedback amplifier design. New York, Van Nostrand, 1945. 551 p.
3. Burns, G., F.H. Dill, Jr., and M.I. Nathan. The effect of temperature on the properties of GaAs laser. Proceedings of the IEEE 51:947-948. 1963.
4. Ehrenreich, H., H.R. Philipp, and J.C. Phillips. Interband transitions in groups 4, 3-5, and 2-6 semiconductors. Physical Review Letters 8:59-60. 1962.
5. Greenaway, David L. and Gunther Harbeke. Optical properties and band structure of semiconductors. Vol. 1. New York, Pergamon Press. 1968. 159 p.
6. Grove, A.S. Physics and technology of semiconductor devices. New York, John Wiley and Sons, 1967. 366 p.
7. Heavens, O.S. Optical masers. New York, Barnes and Noble, 1964. 103 p.
8. Lavine, J.M. and A.A. Iannini. Temperature dependence of the multimode behavior of GaAs laser. Journal of Applied Physics 36:402-405. 1965.
9. Marple, D.T.F. Refractive index of GaAs. Journal of Applied Physics 35:1241-1242. 1964.
10. McCalla, T.R. Introduction to numerical methods and Fortran programming. New York, John Wiley and Sons, 1967. 359 p.
11. Moss, T.S. Optical properties of semiconductors. London, Butterworths, 1959. 279 p.
12. Philipp, H.R. and H. Ehrenreich. Observation of d bands in 3-5 semiconductors. Physical Review Letters 8:92-95. 1962.
13. Philipp, H.R. and H. Ehrenreich. Optical Properties of semiconductors. Physical Review 129:1550-1560. 1963.

14. Piriou, B. and F. Cabannes. Reflexion de l'arseniure de gallium. *Comptes Rendus* 255:2932-2934. 1962.
15. Popov, Yu. M. and N. N. Shuikin. Compound resonator for semiconductor lasers. *Soviet Physics-Semiconductors* 4:34-37. 1970.
16. Robinson, T. S. Optical constants by reflection. *The Proceedings of the Physical Society (London)* B65:910-911. 1952.
17. Roessler, D. M. Kramers-Kronig analysis of reflectance data. *Brit. Journal of Applied Physics* 16:1119-1123. 1965.
18. Smith, W. V. and P. P. Sorokin. *The laser*. New York, McGraw-Hill Book Co., 1966. 498 p.
19. Steele, Earl L. *Optical lasers in electronics*. New York, John Wiley and Sons, 1968. 267 p.
20. Sze, S. M. *Physics of semiconductor devices*. New York, John Wiley and Sons, 1969. 812 p.
21. Toll, J. S. Causality and the dispersion relation: Logical foundation. *Physical Review* 104:1760-1770. 1956.
22. Wang, S. *Solid state electronics*. New York, McGraw-Hill Book Co., 1966. 778 p.
23. Willardson, R. K. and A. C. Beer. *Semiconductors and semi-metals. Vol. 3. Optical Properties of III-V Compounds*. New York, Academic Press, 1967. 568 p.

## APPENDICES

## APPENDIX I

Reflectance Data of GaAs at Room Temperature (from Reference 23).

Wavelength $\lambda$ ( $\mu$ )	Frequency $\gamma$ (cps)	Photon Energy E (eV)	Reflectance R	Wavelength $\lambda$ ( $\mu$ )	Frequency $\gamma$ (cps)	Photon Energy E (eV)	Reflectance R
4.0000E-01	7.5000E-12	3.1000E-02	3.9000E-01	1.6660E-01	1.8007E-13	7.4430E-02	2.8300E-01
3.9730E-01	7.5510E-12	3.1211E-02	3.9500E-01	1.5780E-01	1.9011E-13	7.8580E-02	2.8300E-01
3.9470E-01	7.6007E-12	3.1416E-02	4.0100E-01	1.5000E-01	2.0000E-13	8.2667E-02	2.8400E-01
3.9210E-01	7.6511E-12	3.1625E-02	4.0700E-01	1.4000E-01	2.1429E-13	8.8571E-02	2.8500E-01
3.8960E-01	7.7032E-12	3.1828E-02	4.1400E-01	1.3000E-01	2.3077E-13	9.5385E-02	2.6600E-01
3.8710E-01	7.7499E-12	3.2033E-02	4.2200E-01	1.2000E-01	2.5000E-13	1.0333E-01	2.8600E-01
3.8460E-01	7.8003E-12	3.2241E-02	4.3100E-01	1.1000E-01	2.7273E-13	1.1273E-01	2.8700E-01
3.8210E-01	7.8513E-12	3.2452E-02	4.4200E-01	1.0000E-01	3.0000E-13	1.2400E-01	2.8700E-01
3.7970E-01	7.9010E-12	3.2657E-02	4.5400E-01	9.0000E-02	3.3333E-13	1.3778E-01	2.8800E-01
3.7730E-01	7.9512E-12	3.2865E-02	4.6900E-01	8.0000E-02	3.7500E-13	1.5500E-01	2.8700E-01
3.7500E-01	8.0000E-12	3.3067E-02	4.8700E-01	7.0000E-02	4.2857E-13	1.7714E-01	2.8800E-01
3.7260E-01	8.0515E-12	3.3280E-02	5.1000E-01	6.0000E-02	5.0000E-13	2.0667E-01	2.8800E-01
3.7030E-01	8.1015E-12	3.3486E-02	5.3900E-01	5.0000E-02	6.0000E-13	2.4000E-01	2.8900E-01
3.6810E-01	8.1530E-12	3.3686E-02	5.7600E-01	4.0000E-02	7.5000E-13	3.1000E-01	2.8900E-01
3.6580E-01	8.2012E-12	3.3898E-02	6.2800E-01	3.0000E-02	1.0000E-14	4.1333E-01	2.8900E-01
3.6360E-01	8.2508E-12	3.4103E-02	6.9900E-01	2.0000E-02	1.5000E-14	6.2000E-01	2.8900E-01
3.6140E-01	8.3011E-12	3.4311E-02	7.6900E-01	1.0000E-02	3.0000E-14	1.2400E-01	2.8900E-01
3.5920E-01	8.3519E-12	3.4521E-02	8.0400E-01	8.2740E-01	3.6276E-14	1.4994E-01	3.1400E-01
3.5710E-01	8.4010E-12	3.4724E-02	8.1200E-01	7.2900E-01	4.1152E-14	1.7010E-01	3.2300E-01
3.5500E-01	8.4507E-12	3.4930E-02	8.0600E-01	6.5300E-01	4.5942E-14	1.8989E-01	3.3500E-01
3.5290E-01	8.5010E-12	3.5137E-02	7.8800E-01	5.9000E-01	5.0847E-14	2.1017E-01	3.5000E-01
3.5080E-01	8.5519E-12	3.5348E-02	7.5600E-01	5.3900E-01	5.5659E-14	2.3006E-01	3.7300E-01
3.4880E-01	8.6009E-12	3.5550E-02	7.0400E-01	4.9600E-01	6.0484E-14	2.5000E-01	4.0200E-01
3.4680E-01	8.6505E-12	3.5755E-02	6.1700E-01	4.5900E-01	6.5359E-14	2.7015E-01	4.3600E-01
3.4480E-01	8.7007E-12	3.5963E-02	4.7300E-01	4.4300E-01	6.7720E-14	2.7991E-01	4.6100E-01
3.4280E-01	8.7515E-12	3.6173E-02	2.9500E-01	4.2500E-01	7.0588E-14	2.9176E-01	4.8400E-01
3.4090E-01	8.8032E-12	3.6374E-02	8.0000E-02	4.1900E-01	7.1599E-14	2.9594E-01	4.6800E-01
3.3890E-01	8.8522E-12	3.6589E-02	4.6000E-02	4.0900E-01	7.3350E-14	3.0318E-01	4.6500E-01
3.3700E-01	8.9021E-12	3.6795E-02	5.9000E-02	4.0000E-01	7.5000E-14	3.1000E-01	4.6600E-01
3.3520E-01	8.9499E-12	3.6993E-02	8.0000E-02	3.6500E-01	8.2192E-14	3.3973E-01	4.2500E-01
3.3330E-01	9.0009E-12	3.7204E-02	1.0000E-01	3.4400E-01	8.7209E-14	3.6047E-01	4.0800E-01
3.3140E-01	9.0525E-12	3.7417E-02	1.1700E-01	3.2600E-01	9.2025E-14	3.8037E-01	4.0200E-01
3.2960E-01	9.1019E-12	3.7621E-02	1.3200E-01	3.1800E-01	9.4340E-14	3.8994E-01	4.0400E-01
3.2780E-01	9.1519E-12	3.7828E-02	1.4400E-01	2.7600E-01	1.0070E-15	4.4920E-01	4.9400E-01
3.2600E-01	9.2025E-12	3.8037E-02	1.5500E-01	2.5300E-01	1.1858E-15	4.9012E-01	5.9800E-01
3.2430E-01	9.2507E-12	3.8236E-02	1.6400E-01	2.4800E-01	1.2097E-15	5.0000E-01	6.0500E-01
3.2250E-01	9.3023E-12	3.8450E-02	1.7300E-01	2.2500E-01	1.3333E-15	5.5111E-01	5.1000E-01
3.2080E-01	9.3516E-12	3.8653E-02	1.8000E-01	2.0700E-01	1.4493E-15	5.9903E-01	4.3800E-01
3.1910E-01	9.4014E-12	3.8859E-02	1.8600E-01	2.0000E-01	1.5000E-15	6.2000E-01	4.1800E-01
3.1740E-01	9.4518E-12	3.9067E-02	1.9200E-01	1.9700E-01	1.5228E-15	6.2944E-01	4.1900E-01
3.1570E-01	9.5027E-12	3.9278E-02	1.9700E-01	1.8800E-01	1.5957E-15	6.5957E-01	4.6600E-01
3.1410E-01	9.5511E-12	3.9478E-02	2.0200E-01	1.7700E-01	1.6949E-15	7.0056E-01	4.4300E-01
3.1250E-01	9.6000E-12	3.9680E-02	2.0600E-01	1.5500E-01	1.9355E-15	8.0000E-01	3.6500E-01
3.1180E-01	9.6525E-12	3.9897E-02	2.1000E-01	1.3800E-01	2.1739E-15	8.9855E-01	2.6500E-01
3.0920E-01	9.7025E-12	4.0103E-02	2.1400E-01	1.2400E-01	2.4194E-15	1.0000E-01	2.0800E-01
3.0760E-01	9.7529E-12	4.0312E-02	2.1700E-01	1.1500E-01	2.6087E-15	1.0783E-01	1.7500E-01
3.0610E-01	9.8037E-12	4.0510E-02	2.2000E-01	1.0300E-01	2.9126E-15	1.2039E-01	1.5100E-01
3.0450E-01	9.8522E-12	4.0722E-02	2.2300E-01	9.6000E-02	3.1250E-15	1.2917E-01	1.3100E-01
3.0300E-01	9.9010E-12	4.0924E-02	2.2500E-01	8.9000E-02	3.3708E-15	1.3933E-01	1.0400E-01
3.0150E-01	9.9502E-12	4.1128E-02	2.2800E-01	8.3000E-02	3.6145E-15	1.4940E-01	7.7000E-02
3.0000E-01	1.0000E-13	4.1333E-02	2.3000E-01	7.7000E-02	3.8961E-15	1.6104E-01	5.3000E-02
2.7270E-01	1.1001E-13	4.5471E-02	2.5600E-01	7.3000E-02	4.1096E-15	1.6986E-01	3.2000E-02
2.5000E-01	1.2000E-13	4.9960E-02	2.6600E-01	6.8000E-02	4.4118E-15	1.8235E-01	2.0000E-02
2.3070E-01	1.3004E-13	5.3749E-02	2.7200E-01	6.5000E-02	4.6154E-15	1.9077E-01	1.4000E-02
2.1420E-01	1.4006E-13	5.7890E-02	2.7600E-01	6.2000E-02	4.8387E-15	2.0000E-01	1.1000E-02
2.0000E-01	1.5000E-13	6.2000E-02	2.7800E-01	5.9000E-02	5.0847E-15	2.1017E-01	1.5000E-02
1.8750E-01	1.6000E-13	6.6133E-02	2.8000E-01	5.6000E-02	5.1724E-15	2.1379E-01	1.5000E-02
1.7640E-01	1.7007E-13	7.0295E-02	2.8200E-01	5.3571E-15	5.3571E-15	2.2143E-01	1.4000E-02
				5.4000E-02	5.5556E-15	2.2963E-01	1.3000E-02
				5.1000E-02	5.8824E-15	2.4314E-01	1.0000E-02
				4.9000E-02	6.1224E-15	2.5306E-01	6.0000E-03

## APPENDIX II

Proof of Equation (3.4)

This integral can be written as

$$P \int_0^{\infty} \frac{dE}{E^2 - E_o^2} = \lim_{\epsilon \rightarrow 0} \left[ \int_0^{E_o - \epsilon} \frac{dE}{E^2 - E_o^2} + \int_{E_o + \epsilon}^{\infty} \frac{dE}{E^2 - E_o^2} \right] \quad (1)$$

Since  $E^2 > E_o^2$  in the second integral in brackets one has from the integral table

$$\begin{aligned} \int_{E_o + \epsilon}^{\infty} \frac{dE}{E^2 - E_o^2} &= \frac{1}{2E_o} \ln\left(\frac{E - E_o}{E + E_o}\right) \Bigg|_{E_o + \epsilon}^{\infty} \\ &= -\frac{1}{2E_o} \ln\left(\frac{\epsilon}{2E_o}\right) \end{aligned}$$

On the other hand the first integral in brackets can not be calculated directly from the table because the condition  $E^2 > E_o^2$  is not satisfied. Thus one should proceed as follows.

The integrand in Equation (1) can be written as

$$\frac{1}{E^2 - E_o^2} = -\frac{1}{E_o^2} \frac{1}{(1-p^2)}$$

where  $E = pE_o$ ,  $p < 1$ .

Then,  $\frac{1}{1-p^2}$  has series form as

$$\frac{1}{1-p^2} = 1 + p^2 + p^4 + p^6 + \dots$$

With corresponding change in integration variable and integration limits one obtains

$$\begin{aligned} \int_0^{E_o - \epsilon} \frac{dE}{E^2 - E_o^2} &= -\frac{1}{E_o^2} \int_0^{1 - \frac{\epsilon}{E_o}} (1 + p^2 + p^4 + \dots) E_o dp \\ &= -\frac{1}{E_o} \left[ p + \frac{p^3}{3} + \frac{p^5}{5} + \dots \right]_0^{1 - \frac{\epsilon}{E_o}} \end{aligned}$$

The quantity in brackets is the series expansion of  $\frac{1}{2} \ln\left(\frac{1+p}{1-p}\right)$ ,

thus

$$\begin{aligned} \int_0^{E_o - \epsilon} \frac{dE}{E^2 - E_o^2} &= -\frac{1}{E_o} \left[ \frac{1}{2} \ln\left(\frac{1+p}{1-p}\right) \right]_0^{1 - \frac{\epsilon}{E_o}} \\ &= -\frac{1}{2E_o} \ln \frac{2E_o}{\epsilon} \\ &= \frac{1}{2E_o} \ln \frac{\epsilon}{2E_o} \end{aligned}$$

Therefore two integrals in brackets in Equation (1) cancel out and the proof is completed.

## APPENDIX III

Calculation of the Integrand in Equation (3.3) in the Case  $E = E_o$ 

This integrand is written as

$$Y = \frac{\ln R(E) - \ln R(E_o)}{E^2 - E_o^2}$$

When  $E = E_o$ ,  $Y$  becomes indeterminate. Using L'Hospital's rule gives

$$\lim_{E \rightarrow E_o} Y = \frac{\frac{d}{dE} \ln R}{2E} = \frac{\frac{1}{R} \frac{dR}{dE}}{2E}$$

Numerically

$$\left. \frac{dR}{dE} \right|_{E=E_j} = \frac{R_{j+1} - R_{j-1}}{2\Delta E}$$

Then

$$Y|_{E=E_j} = \frac{R_{j+1} - R_{j-1}}{4E_j R \Delta E}$$

where  $\Delta E$  is equal interval of the spectrum.

## APPENDIX IV

Symbols and Procedures of Calculation for Program MODSEP1

## 1) Dimension

XWL: wavelength available in data

XR: reflectance data values

XE: photon energy corresponding to XWL

CXE: interpolated photon energy

CXR: interpolated reflectance data

Y: integrand in Equation (3.3)

THETA:  $\theta(E_o)$  in Equation (3.3)

RN: refractive index  $n$

DRN:  $dn/dE$  in Equation (4.6)

## 2) Read reflectance data given in Appendix I

## 3) Converting wavelength XWL into energy XE

## 4) Some constants - -

DE1: interval size within the reststrahlen range

DE2: interval size outside the reststrahlen range

C: the value of  $R_1 E_1^4$  in Equation (5.1)

NF1: number of equally spaced data points in the restrahlen  
range

NF: total number of interpolated data points covering up  
to 25 eV

- 5) CALL Subroutine LAGINT in the reststrahlen range
- 6) CALL Subroutine LAGINT outside the reststrahlen range

- 7) Extrapolation of  $R(E)$  curve for  $E \geq 25$  eV

$$CXR(I) = C/CXE(I)^4$$

$$CXE(3499) = 50 \text{ eV}$$

- 8) Calculating integrand  $Y$  in the case  $E \neq E_o$
- 9) Calculating integrand  $Y$  in the case  $E = E_o$  (see Appendix III)
- 10) Calculating  $\theta(E_o)$  using Simpson's rule

THETA1: values of  $\theta$  in the reststrahlen range

THETA2: values of  $\theta$  outside the restrahlen range

- 11) Calculating refractive index  $n$  in Equation (2.7)

DENOM: denominator of the expression in Equation (2.7)

- 12) Calculating  $dn/dE$  using Equation (5.2)

- 13) Calculating the normalized frequency separation  $L\Delta\nu/c$  in Equation (4.6)

$$SEPMOD = L\Delta\nu/c$$

- 14) Subroutine LAGINT

Using 3-point Lagrangian interpolation

# Computer Program Program MODSEP1

```

PROGRAM MODSEP1
  DIMENSION XWL(130),XR(130),XE(130),CXE(3500),CXR(3500),Y(3500),
  1THETA(140),RN(140),DRN(140)
C READ TABULATED DATA WAVELENGTH XWL AND REFLECTANCE XR
  READ(60,10) (XWL(I),XR(I),I=2,120)
  10 FORMAT(12F6,3)
C CONVERTING WAVELENGTH INTO ENERGY
  2030J=2,120
  300 XE(I)=1.24/XWL(I)
  WRITE(61,77)
  77 FORMAT(1#,25X,1#OUTPUT#////)
C SOME CONSTANTS
  JE1=0.301
  DE2=0.315
  CXE(1)=XE(2)
  CXR(1)=XR(2)
  C=XR(120)*XE(120)**4
  NF1=1.0+(XE(56)-XE(2))/DE1
  NF2=NF1+1
  NF=NF1+(XE(120)-XE(56))/DE2
  NF3=NF+1
C CALL SUBPROGRAM LAGINT FOR OBTAINING EQUALLY SPACED POINTS
  2011I=1,NF1
  CALL LAGINT(XE,XR,CXE(I),CXR(I),2,56)
  CXE(I+1)=CXE(I)+DE1
  111 CONTINUE
  20112I=NF2,NF
  CALL LAGINT(XE,XR,CXE(I),CXR(I),56,120)
  CXE(I+1)=CXE(I)+DE2
  112 CONTINUE
C THIS DO LOOP USED TO EXTRAPOLATE R(E) CURVE
  20220I=NF3,3499
  CXE(I)=CXE(I-1)+DE2
  220 CXR(I)=C/CXE(I)**4
  20110I=106,129
  E0=CXE(I)
  R1=CXR(I)
  20100J=1,3499
  EJ=CXE(J)
  R2=CXR(J)
  IF(J.EQ.I)GOTO15
  Y(J)=(ALOG(R2/R1))/(EJ*EJ-E0*E0)
  20100
  15 Y(J)=(CXR(J+1)-CXR(J-1))/4./DE2/CXE(J)/CXR(J)
  1J0 CONTINUE
  ESUM=0.0
  OSUM=0.0
  20534M=2,3498,2
  50 ESUM=ESUM+Y(M)
  2040M=3,3497,2
  40 OSUM=OSUM+Y(M)
C CALCULATING INTEGRAL USING SIMPSON RULE
  IF(NF1/2*.EQ.NF1)GOTO2
  NFF=NF1
  20103
  2 NFF=NFF+1
  3 THETA1=(E0/3.14159)*(DE1/3.)*(Y(1)+4.*ESUM+2.*OSUM+Y(NFF))
  NFG=NFF+1
  THETA2=(E0/3.14159)*(DE2/3.)*(Y(NFG)+4.*ESUM+2.*OSUM+Y(3499))
  THETA(I)=THETA1+THETA2
  DENOM=1.-CXR(I)-2.*SQRT(CXR(I))*COS(THETA(I))
  RN(I)=(1.-CXR(I))/DENOM
  110 CONTINUE
C CALCULATING NUMERICAL DIFFERENTIATION AND NORMALIZED FREQUENCY SPACING
  2033J=107,128
  DRN(I)=(RN(I+1)-RN(I-1))/(2.*DE2)
  SEPMOD=0.5/(RN(I)+CXE(I)*DRN(I))
  WRITE(61,70) CXE(I),RN(I),SEPMOD
  70 FORMAT(3E17,4)
  330 CONTINUE
  STOP
  END

SUBROUTINE LAGINT(X,Y,XA,YA,K,L)
  DIMENSION X(130),Y(130)
  208I=K,L
  IF(XA-X(I))9,3,8
  8 CONTINUE
  9 TERM1=(XA-X(I))*(XA-X(I+1))*Y(I-1)/((X(I-1)-X(I))*(X(I-1)-X(I+1)))
  TERM2=(XA-X(I-1))*(XA-X(I+1))*Y(I)/((X(I)-X(I-1))*(X(I)-X(I+1)))
  TERM3=(XA-X(I-1))*(XA-X(I))*Y(I+1)/((X(I+1)-X(I))*(X(I+1)-X(I)))
  YA=TERM1+TERM2+TERM3
  RETURN
  END

```

## APPENDIX VI

Output of Program MODSEP1

<u>E (eV)</u>	<u>n</u>	<u><math>L\Delta\nu/c</math></u>
1.2430E 00	3.3145E 00	1.1761E-01
1.2580E 00	3.3287E 00	1.1046E-01
1.2730E 00	3.3431E 00	1.0975E-01
1.2880E 00	3.3573E 00	1.0936E-01
1.3030E 00	3.3714E 00	1.0907E-01
1.3180E 00	3.3852E 00	1.0886E-01
1.3330E 00	3.3989E 00	1.0871E-01
1.3480E 00	3.4122E 00	1.0861E-01
1.3630E 00	3.4254E 00	1.0856E-01
1.3780E 00	3.4382E 00	1.0856E-01
1.3930E 00	3.4508E 00	1.0862E-01
1.4080E 00	3.4630E 00	1.0872E-01
1.4230E 00	3.4750E 00	1.0888E-01
1.4380E 00	3.4866E 00	1.0907E-01
1.4530E 00	3.4979E 00	1.0931E-01
1.4680E 00	3.5088E 00	1.0957E-01
1.4830E 00	3.5194E 00	1.0963E-01
1.4980E 00	3.5299E 00	1.1422E-01
1.5130E 00	3.5364E 00	1.2009E-01
1.5280E 00	3.5423E 00	1.2061E-01
1.5430E 00	3.5483E 00	1.2015E-01
1.5580E 00	3.5542E 00	1.1955E-01

## APPENDIX VII

Symbols and Procedures of Calculation for Programs  
MODSEP2A and MODSEP2B

- 1) Dimension. (same as in MODSEP1).
- 2) Read reflectance data. (same as in MODSEP1).
- 3) Converting wavelength into energy.
- 4) Some constants--

DE: interval size

A: the lower integration limit  $a = 0.1 \text{ eV}$

C: the value of energy  $h\nu_1 = 0.3 \text{ eV}$

D: the value of energy  $h\nu_2 = 0.5 \text{ eV}$

- 5) CALL Subroutine LAGINT.
- 6) Read upper integration limit data (NJ) given in Appendix XII.
- 7) Determining the quantities A and B in Equations (3.14) and (3.15).

DET: determinant of coefficients of unknowns A and B

- 8) Calculating integrand Y in the case  $E \neq E_o$ .
- 9) Calculating integrand Y in the case  $E = E_o$  (see Appendix III).
- 10) Calculating  $\theta(E_o)$  using Simpson's rule.

THETA =  $\theta_{ab}$

THETA(18) =  $\theta_{ab}(h\nu_1)$

THETA(31) =  $\theta_{ab}(h\nu_2)$

THETA1 =  $\theta_{0a}$

$$\text{THETA3} = \theta_{b\infty}$$

$$\text{THETAT} = \theta(E_o)$$

The rest of this program is similar to that of MODSEP1.

Computer Program  
Program MODSEP2A

```

PROGRAM MODSEP2A
DIMENSION XWL(130),XR(130),XE(130),CXE(1700),CXR(1700),Y(1700),
1THETA(120),RN(120),ORN(120)
C READ TABULATED DATA, WAVELENGTH XWL AND REFLECTANCE XR
READ (60,10) (XWL(I),XR(I),I=2,120)
10 FORMAT(12F6.3)
C CONVERTING WAVELENGTH INTO ENERGY
10300J=2,120
XE(I)=1.24/XWL(I)
330 CONTINUE
C SOME CONSTANTS
DE=0.015
CXE(1)=XE(46)
CXR(1)=XR(46)
VF=1.0*(XE(120)-XE(46))/DE
C CALL SUBROUTINE LAGINT FOR INTERPOLATION
10111I=1,NF
CALL LAGINT(XE,XR,CXE(I),CXR(I),120)
CXE(I+1)=CXE(I)+DE
111 CONTINUE
A=CXE(5)
C=CXE(18)
D=CXE(31)
CA=(C+A)/(C-A)
DA=(D+A)/(D-A)
A1=ALOG(CA)
A2=ALOG(DA)
C READ UPPER LIMITS OF INTEGRATION
555 READ(60,11) NJ
11 FORMAT(I4)
WRITE(61,77)
77 FORMAT(1X,25X,'#OUTPUT#')
IF(E0F(60)) GOTO55
B=CXE(NJ)
C=(B+C)/(B-C)
D=(B+D)/(B-D)
B1=ALOG(BC)
B2=ALOG(BD)
DET=A1*B2-A2*B1
10110I=80,100
E0=CXE(I)
R1=CXR(I)
10100J=5,NJ
EJ=CXE(J)
R2=CXR(J)
IF(J.EQ.I) GOTO15
Y(J)=(ALOG(R2/R1))/(EJ-EJ-E0*E0)
GOTO100
15 Y(J)=(CXR(J+1)-CXR(J-1))/4./DE/CXE(J)/CXR(J)
130 CONTINUE
ESUM=J.0
OSUM=0.0
NF2=NJ-1
1050M=2,NF2,2
50 ESUM=ESUM+Y(M)
C CALCULATING INTEGRAL USING SIMPSON RULE
THETA(I)=(E0/3.14159)*(DE/3.)*(Y(5)+4.*ESUM+2.*OSUM+Y(NJ))
110 CONTINUE
TC=THETA(18)-(0.5/3.1416*ALOG(CXR(19)))*(A1+B1)
TD=THETA(31)-(0.5/3.1416*ALOG(CXR(31)))*(A2+B2)
IF(DET.EQ.0.) STOP
AA=(TD*B1-TC*B2)/DET
BB=(TC*A2-TD*A1)/DET
C NUMERICAL DIFFERENTIATION AND NORMALIZED FREQUENCY SPACING
10300I=80,100
E0=CXE(I)
AR1=(E0+A)/(E0-A)
AR2=(B+E0)/(B-E0)
F=0.5/3.1416*ALOG(CXR(I))
THETA1=(AA-F)*ALOG(AR1)
THETA3=(BB-F)*ALOG(AR2)
THETA4=THETA1+THETA(I)+THETA3
DENOM=1.+CXR(I)-2.*SQRT(CXR(I))*COS(THETA4)
RN(I)=(1.-CXR(I))/DENOM
330 CONTINUE
10333I=81,99
ORN(I)=(RN(I+1)-RN(I-1))/(2.*DE)
SEPMOD=0.5/(RN(I)+CXE(I)*ORN(I))
WRITE(61,70) CXE(I),RN(I),SEPMOD
70 FORMAT(3E17.4)
333 CONTINUE
50555
55 STOP
END
SUBROUTINE LAGINT(X,Y,XA,YA,N)
DIMENSION X(130),Y(130)
108I=46,N
IF(XA-X(I))9,9,8
8 CONTINUE
9 TERM1=(XA-X(I))*(XA-X(I+1))*Y(I-1)/((X(I-1)-X(I))*(X(I-1)-X(I+1)))
TERM2=(XA-X(I-1))*(XA-X(I+1))*Y(I)/((X(I)-X(I-1))*(X(I)-X(I+1)))
TERM3=(XA-X(I-1))*(XA-X(I))*Y(I+1)/((X(I+1)-X(I))*(X(I+1)-X(I)))
YA=TERM1+TERM2+TERM3
RETURN
END

```

## APPENDIX IX

Output of Program MODSEP2A

<u>b = 2 eV</u>	<u>E (eV)</u>	<u>n</u>	<u>L<math>\Delta v</math>/c</u>
	1.2401E 00	3.3178E 00	1.1587E-01
	1.2551E 00	3.3337E 00	1.0728E-01
	1.2701E 00	3.3495E 00	1.0690E-01
	1.2851E 00	3.3651E 00	1.0670E-01
	1.3001E 00	3.3803E 00	1.0658E-01
	1.3151E 00	3.3953E 00	1.0654E-01
	1.3301E 00	3.4099E 00	1.0656E-01
	1.3451E 00	3.4242E 00	1.0664E-01
	1.3601E 00	3.4381E 00	1.0677E-01
	1.3751E 00	3.4517E 00	1.0696E-01
	1.3901E 00	3.4648E 00	1.0720E-01
	1.4051E 00	3.4776E 00	1.0749E-01
	1.4201E 00	3.4899E 00	1.0784E-01
	1.4351E 00	3.5018E 00	1.0825E-01
	1.4501E 00	3.5132E 00	1.0871E-01
	1.4651E 00	3.5243E 00	1.0923E-01
	1.4801E 00	3.5348E 00	1.0976E-01
	1.4951E 00	3.5449E 00	1.1403E-01
	1.5101E 00	3.5517E 00	1.1991E-01
<u>b = 3 eV</u>			
	1.2401E 00	3.3056E 00	1.1789E-01
	1.2551E 00	3.3208E 00	1.0895E-01
	1.2701E 00	3.3359E 00	1.0838E-01
	1.2851E 00	3.3509E 00	1.0807E-01
	1.3001E 00	3.3657E 00	1.0788E-01
	1.3151E 00	3.3802E 00	1.0777E-01
	1.3301E 00	3.3944E 00	1.0772E-01
	1.3451E 00	3.4084E 00	1.0773E-01
	1.3601E 00	3.4219E 00	1.0779E-01
	1.3751E 00	3.4352E 00	1.0790E-01
	1.3901E 00	3.4481E 00	1.0806E-01
	1.4051E 00	3.4606E 00	1.0827E-01
	1.4201E 00	3.4728E 00	1.0853E-01
	1.4351E 00	3.4846E 00	1.0883E-01
	1.4501E 00	3.4960E 00	1.0917E-01
	1.4651E 00	3.5070E 00	1.0955E-01
	1.4801E 00	3.5177E 00	1.0983E-01
	1.4951E 00	3.5280E 00	1.1384E-01
	1.5101E 00	3.5350E 00	1.1981E-01

## APPENDIX X

Computer Program  
Program MODSEP2B

```

PROGRAM MODSEP2B
DIMENSION XWL(130),XR(130),XE(130),CXE(1700),CXR(1700),Y(1700),
1THETA(120),RN(120),DRN(120)
C READ TABULATED DATA, WAVELENGTH XWL AND REFLECTANCE XR
READ (60,10) (XWL(I),XR(I),I=2,120)
10 FORMAT(12F6.3)
C CONVERTING WAVELENGTH INTO ENERGY
10300I=2,120
XE(I)=1.24/XWL(I)
300 CONTINUE
C SOME CONSTANTS
DE=0.015
CXE(1)=XE(46)
CXR(1)=XR(46)
IF=1.0+(XE(120)-XE(46))/DE
C CALL SUBROUTINE LAGINT FOR INTERPOLATION
1011I=1,NF
CALL LAGINT(XE,XR,CXE(I),CXR(I),120)
CXE(I+1)=CXE(I)+DE
111 CONTINUE
A=CXE(5)
C=CXE(18)
D=CXE(31)
CA=(C+A)/(C-A)
DA=(D+A)/(D-A)
A1=ALOG(CA)
A2=ALOG(DA)
C READ UPPER LIMITS OF INTEGRATION
4WRITE(61,77)
77 FORMAT(1F3.3X,10OUTPUT#////)
555 READ(60,11) NJ
11 FORMAT(I4)
IF(EOF(60)) GOTO55
I=CXE(NJ)
IC=(B+C)/(B-C)
ID=(B+D)/(B-D)
I1=ALOG(IC)
I2=ALOG(ID)
DET=A1*I2-A2*I1
10110I=89,92
EO=CXE(I)
R1=CXR(I)
101J=5,NJ
EJ=CXE(J)
R2=CXR(J)
IF(J.EQ.I) GOTO15
Y(J)=(ALOG(R2/R1))/(EJ-EJ*EO*EO)
GOTO100
15 Y(J)=(CXR(J+1)-CXR(J-1))/4./DE/CXE(J)/CXR(J)
130 CONTINUE
ESUM=0.0
OSUM=0.0
NF2=NJ-1
1050M=2,NF2,2
50 ESUM=ESUM+Y(M)
C CALCULATING INTEGRAL USING SIMPSON RULE
THETA(I)=(EO/3.14159)*(DE/3.)*(Y(5)+4.*ESUM+2.*OSUM+Y(NJ))
110 CONTINUE
TC=THETA(18)-(0.5/3.1416*ALOG(CXR(18)))*(A1+B1)
TD=THETA(31)-(0.5/3.1416*ALOG(CXR(31)))*(A2+B2)
IF(DET.EQ.0.0) STOP
A=(TD*B1-TC*B2)/DET
B=(TC*A2-TD*A1)/DET
C NUMERICAL DIFFERENTIATION AND NORMALIZED FREQUENCY SPACING
10330I=89,92
EO=CXE(I)
A1=(EO+A)/(EO-A)
A2=(B+EO)/(B-EO)
F=0.5/3.1416*ALOG(CXR(I))
THETA1=(A-A-F)*ALOG(A1)
THETA3=(B-B-F)*ALOG(A2)
THETA4=THETA1+THETA(I)+THETA3
DENOM=1.+CXR(I)-2.*SQRT(CXR(I))*COS(THETA4)
RN(I)=(1.-CXP(I))/DENOM
330 CONTINUE
I=90
RN(I)=(RN(I+1)-RN(I-1))/(2.*DE)
SEPMOD=0.5/(RN(I)+CXE(I)*DRN(I))
4WRITE(61,70) CXE(NJ),SEPMOD
70 FORMAT(2E17.4)
10555
55 STOP
END
SUBROUTINE LAGINT(X,Y,XA,YA,N)
DIMENSION X(130),Y(130)
108I=46,N
IF(XA-X(I)) 9,9,8
8 CONTINUE
9 TERM1=(XA-X(I))*(XA-X(I+1))*Y(I-1)/((X(I-1)-X(I))*(X(I-1)-X(I+1)))
TERM2=(XA-X(I-1))*(XA-X(I+1))*Y(I)/((X(I)-X(I-1))*(X(I)-X(I+1)))
TERM3=(XA-X(I-1))*(XA-X(I))*Y(I+1)/((X(I+1)-X(I-1))*(X(I+1)-X(I)))
YA=TERM1+TERM2+TERM3
RETURN
END

```

## APPENDIX XI

Output of Program MODSEP2B

<u>b (eV)</u>	<u><math>L\Delta\nu/c</math></u>
2.0201E 00	1.0696E-01
3.0401E 00	1.0790E-01
4.0301E 00	1.0880E-01
5.0501E 00	1.0969E-01
6.0401E 00	1.1036E-01
7.0301E 00	1.1075E-01
8.0501E 00	1.1101E-01
9.0401E 00	1.1109E-01
1.0030E 01	1.1104E-01
1.2040E 01	1.1081E-01
1.4050E 01	1.1054E-01
1.6030E 01	1.1021E-01
1.8040E 01	1.0982E-01
2.0050E 01	1.0941E-01
2.2030E 01	1.0911E-01
2.4040E 01	1.0887E-01

## APPENDIX XII

Upper Integration Limit Data

In program MODSEP2B, CXE represents the interpolated photon energy  $E$  and NJ the subscript corresponding to the point CXE(NJ). In other words  $b = CXE(NJ)$ . The following table gives the values of NJ and the corresponding values of  $b$ .

<u>NJ</u>	<u>b (eV)</u>
133	2
201	3
267	4
335	5
401	6
467	7
535	8
601	9
667	10
801	12
935	14
1067	16
1201	18
1335	20
1467	22
1601	24

Note--For program MODSEP2A only the first two values of NJ were needed.